

# Excimer laser ablation of sintered hydroxyapatite

Kazuhiro Nakata\*, Masahiro Umehara, Takuya Tsumura

Joining and Welding Research Institute, Osaka University, 11-1, Mihogaoka, Ibaraki, Osaka, 567-0047, Japan

Available online 23 August 2006

## Abstract

The ablation treatment of a sintered hydroxyapatite ( $\text{Ca}_{10}(\text{PO}_4)_6(\text{OH})_2$ ) sample has been studied by irradiating the excimer laser in air at one atmosphere for the micro machining treatment. Three different excimer lasers of ArF, KrF and XeF with wavelengths of 193 nm, 248 nm and 351 nm, respectively were used to examine the effect of the wavelength on the ablation rate and the surface morphology of the ablated area. Photochemical ablation of sintered hydroxyapatite is possible with ArF and KrF excimer lasers and the flat bottom shape of an ablated hole with sharp edge can be obtained. On the contrary, thermal ablation occurred in the case of XeF laser due to a long wavelength, and the ablation rate was much larger than those in the case of ArF and KrF lasers, though the ablated surface was rough and not flat. Threshold values of laser fluence for ablation were about 0.8, 1.5 and 6  $\text{J}/\text{cm}^2$  for ArF, KrF and XeF, respectively.

© 2006 Elsevier B.V. All rights reserved.

PACS: 52.38Mf

Keywords: Hydroxyapatite; Laser ablation; Excimer laser; Surface morphology; Ablation rate; Threshold fluence

## 1. Introduction

Hydroxyapatite (HA) is a well-known bioactive ceramic as biomaterials. However, due to brittle property inherent to ceramics material, machining and shaping of HA is difficult. Laser ablation by using ultraviolet laser has high potential for micro machining of the variety of materials. Research works [1–7] on laser ablation of HA by excimer laser with ultraviolet wavelength have been reported, but they were related to laser ablation plume behavior [1,2,4] and thin film coating of hydroxyapatite [3,5–7].

In this study, the fine surface modification treatment intended to micro machining by using excimer laser ablation of sintered hydroxyapatite has been evaluated with three excimer lasers of ArF, KrF and XeF with different wavelengths. Ablation rate and threshold laser energy for ablation as well as fine surface morphology of ablated area were evaluated by changing laser ablation fluence for each excimer laser.

## 2. Experimental conditions

Commercially available Hydroxyapatite ( $\text{Ca}_{10}(\text{PO}_4)_6(\text{OH})_2$ ) sintered sample, which was sintered at 1373 K for 10.8 ks, was used. Shape and size of the specimen is a tablet with 13 mm in

diameter and 3.6 mm in thickness, and its surface was polished with #3  $\mu\text{m}$  diamond paste. Relative density of Sintered sample is 99.3% and mol ratio of Ca/P is 1.67.

Excimer laser apparatus (Lumonics, PM-886) was used for ablation treatment with three excimer lasers, ArF, KrF and XeF. The wavelengths of these excimer lasers are 193 nm, 248 nm and 351 nm, respectively. Pulse irradiation time is 15 ns. A laser beam was used to irradiate vertically on the specimen surface and focused by quartz glass lens at the area of 0.3 mm in diameter on its surface in air under normal atmospheric pressure. Irradiated laser energy per  $\text{cm}^2$  (laser fluence) was changed at the range of 0.7 to 4.0, 0.9 to 9.8 and 1.8 to 9.1  $\text{J}/\text{cm}^2$  for ArF, KrF and XeF lasers, respectively. Constant repetition rate of 10 Hz and the number of shot of 100 were used.

After ablation treatment, the specimen surface was gold plated in vacuum evaporation, and then surface morphology was observed with scanning electron microscope (SEM) with energy dispersed type X-ray analyzer (EDX). The depth profile of an ablation hole was measured by a contact instrument for surface roughness.

## 3. Results and discussions

### 3.1. Surface morphology

Figs. 1, 2 and 3 show the surface morphologies of laser ablated areas irradiated by ArF at 4.0  $\text{J}/\text{cm}^2$ , KrF at 6.6  $\text{J}/\text{cm}^2$  and

\* Corresponding author. Tel.: +81 6 6879 8656; fax: +81 6 6879 8689.

E-mail address: [nakata@jwri.osaka-u.ac.jp](mailto:nakata@jwri.osaka-u.ac.jp) (K. Nakata).

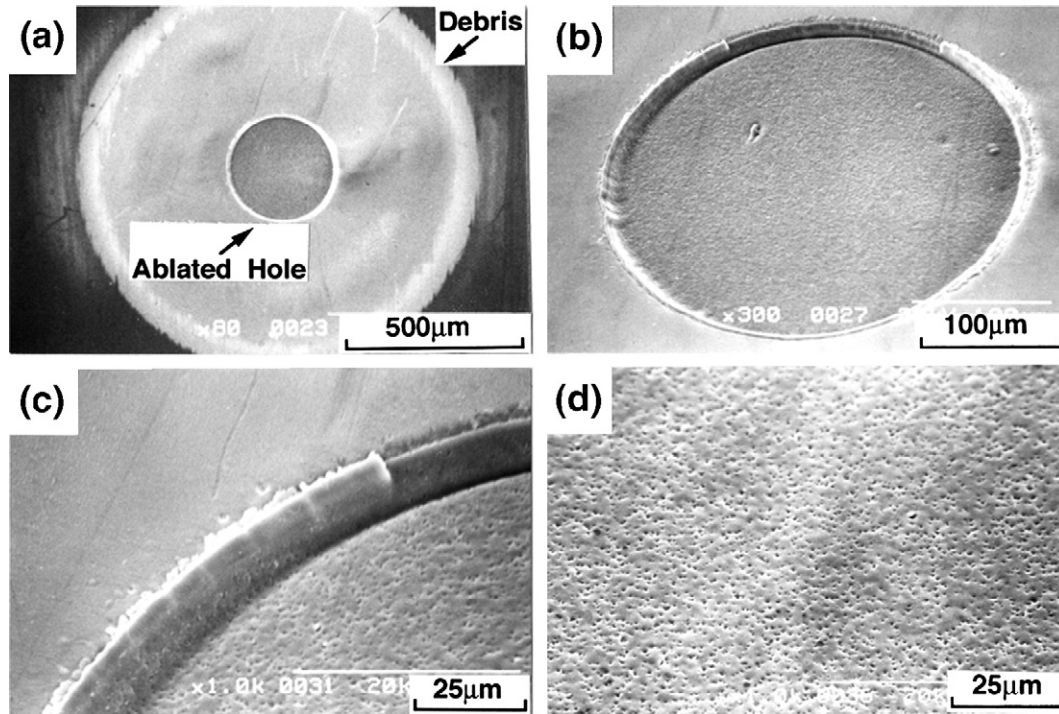


Fig. 1. Surface morphology of ArF laser irradiated area of hydroxyapatite at  $4.0 \text{ J/cm}^2$ , 10 Hz, 100 shots, in air of 1 atmosphere; (a) Appearance of ablated area with debris, (b) Ablated hole, (c) Edge of ablated hole, (d) Surface of the central area of the ablated hole.

XeF at  $9.1 \text{ J/cm}^2$ , respectively. (a), (b), (c) and (d) in each figure show the appearance of an ablated area from the vertical view to the specimen surface, an ablated hole, the edge of the hole and the surface morphology of the central area of the hole bottom from tilted angle view. In (a) of each figure a central circle area is

an ablated hole and surrounding circle area is debris, which was evaporated from an ablated hole and deposited around the hole. Large differences in the sharpness of the hole edge and the roughness of the hole bottom surface are apparently observed depending on the wavelength of the excimer laser. By ArF

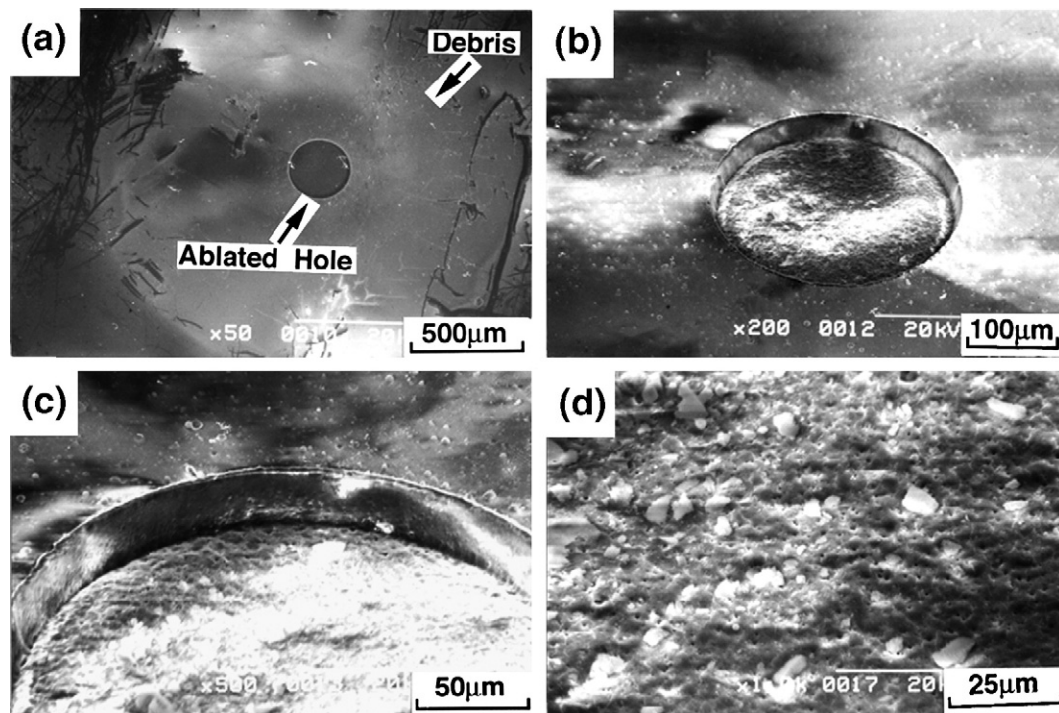


Fig. 2. Surface morphology of KrF laser irradiated area of hydroxyapatite at  $6.6 \text{ J/cm}^2$ , 10 Hz, 100 shots, in air of 1 atmosphere; (a) Appearance of ablated area with debris, (b) Ablated hole, (c) Edge of ablated hole, (d) Surface of the central area of the ablated hole.

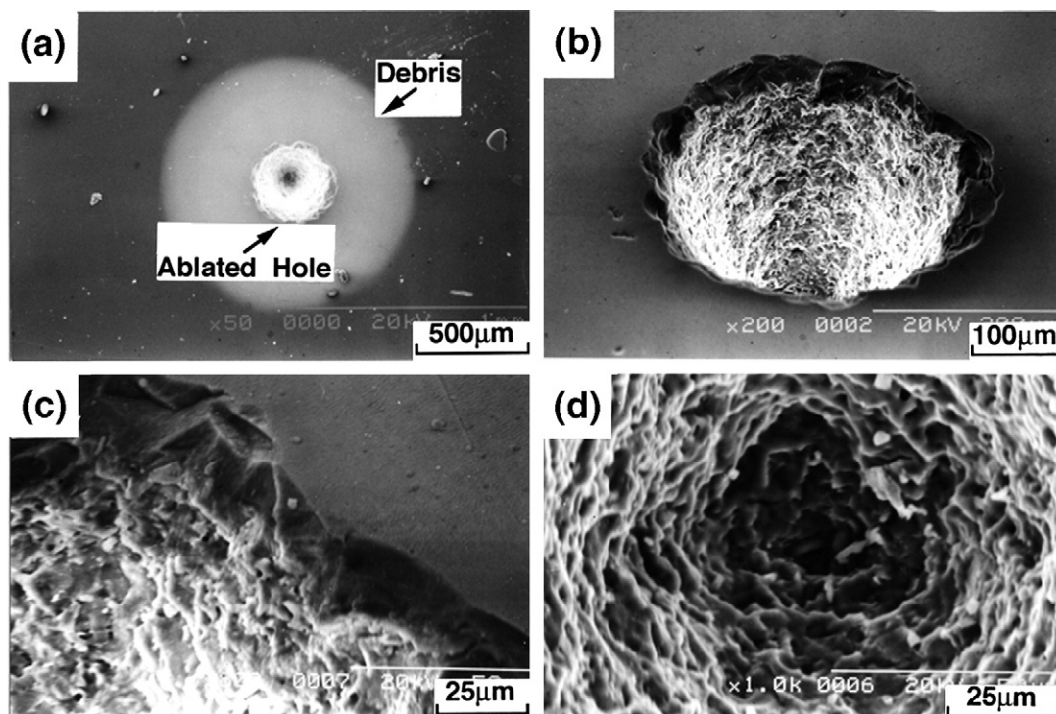


Fig. 3. Surface morphology of XeF laser irradiated area of hydroxyapatite at  $9.1 \text{ J/cm}^2$ , 10 Hz, 100 shots, in air of 1 atmosphere; (a) Appearance of ablated area with debris, (b) Ablated hole, (c) Edge of ablated hole, (d) Surface of the central area of the ablated hole.

excimer laser irradiation, a sharp edge and the smooth and flat surface of the hole can be obtained. Similar sharp edge and flat surface of the hole can be obtained by KrF laser, but the surface is more rough comparing with ArF laser due to small particles or projections, which were not observed at ArF laser. In both lasers, cracking was not observed at the ablated area of the specimen. On the contrary, by XeF laser irradiation, the edge of the hole was not sharp with an irregular shape due to the cracking at the edge of the hole. In addition, the bottom of the hole was much rough and not flat, and showed the apparent feature of melting. These differences in surface morphology are clearly seen in the depth profiles of the laser irradiated zone as shown in Fig. 4(a), (b) and (c) for ArF, KrF and XeF, respectively.

### 3.2. Ablation rate and threshold fluence for ablation

Fig. 5 shows the effect of the laser fluence on the ablation depth by different excimer lasers. The critical energy to be able

to ablate a sintered hydroxyapatite, that is, threshold fluence is clearly observed in Fig. 5 and is shown in Fig. 6 against the wavelength of each excimer laser. The threshold fluence decreased with decreasing wavelength, and XeF showed extremely large value. Ablation depth increases almost linearly with increasing laser fluence excepting small fluence near the threshold value. The ablation rate, which means the increasing rate of ablation depth to laser fluence, was approximately 0.1, 0.2 and  $28 \mu\text{m/J/cm}^2$  for ArF, KrF and XeF lasers, respectively. It increased with increasing wavelength of the excimer laser, but XeF laser showed extremely high rate. Thus, XeF laser apparently showed different phenomena in ablation comparing with ArF and KrF lasers.

### 3.3. Discussion

Fig. 7 shows chemical bond energy of major composition of hydroxyapatite as well as the typical organic components of the

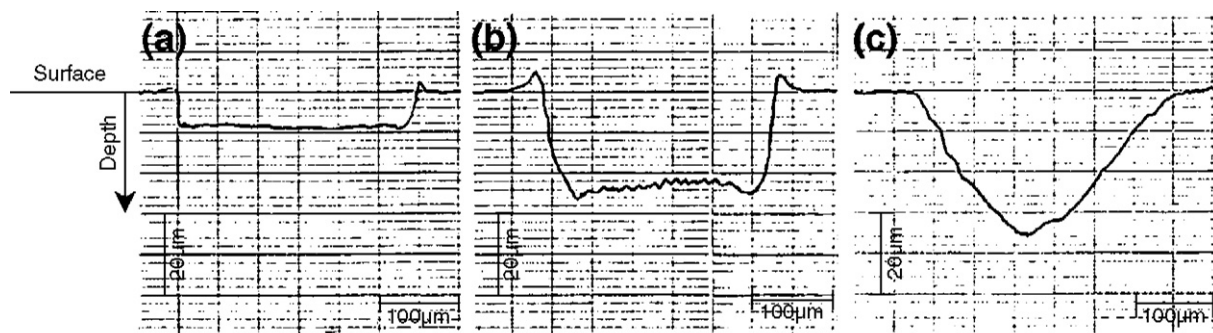


Fig. 4. Depth profiles of laser ablated hole at 10 Hz, 100 shots; (a) ArF:  $4.0 \text{ J/cm}^2$ , (b) KrF:  $9.8 \text{ J/cm}^2$ , (c) XeF:  $7.3 \text{ J/cm}^2$ .

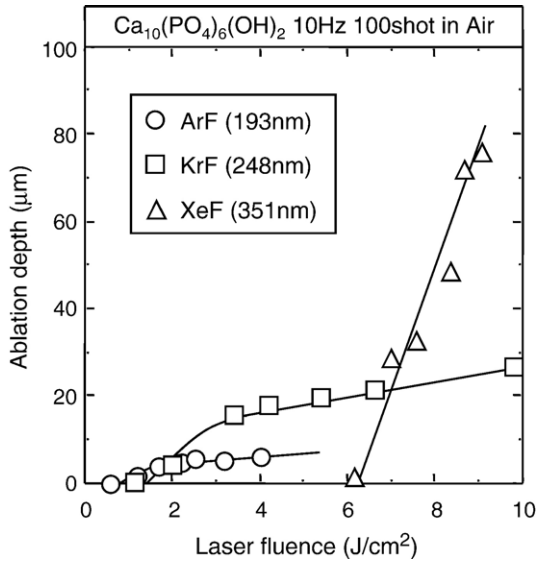


Fig. 5. Effect of laser fluence on the ablation depth by different excimer lasers of ArF, KrF and XeF.

bone in comparison with photon energy of each excimer laser in single energy level, 6.4, 5.0 and 3.5 eV for ArF, KrF and XeF, respectively [8]. ArF laser has higher photon energy than chemical bond energies of P–O, P=O and Ca–O. Therefore, most of the composition of hydroxyapatite can be ablated photochemically by direct cutting of each chemical bond with almost no thermal influence. This resulted in the sharp edge and very smooth surface of the ablated hole. KrF has also high photon energy, but can ablate photochemically by cutting only the Ca–O bond. Thus, its effect will be limited because the bond energies of the other bonds are higher than KrF photon energy. Therefore, not only photochemical ablation but also thermal ablation occurred and this resulted in the increase of the ablation rate. Thus, comparably rough surface was made due to the formation of small particles or projections. S. Fujisaka et al. [9] reported 0.3–0.5 J/cm<sup>2</sup> as the threshold fluence of bones

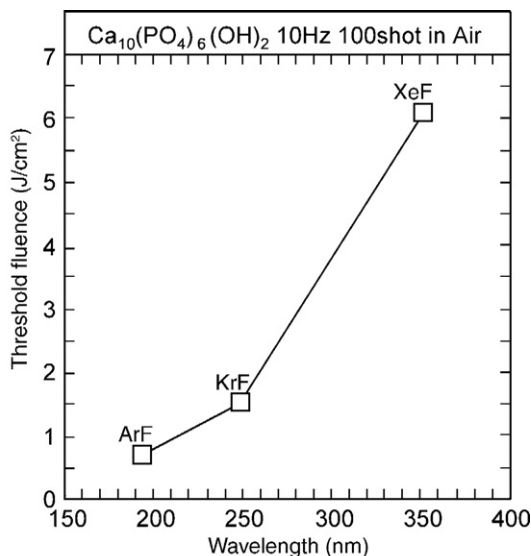


Fig. 6. Relation between threshold fluence and wavelength of excimer laser.

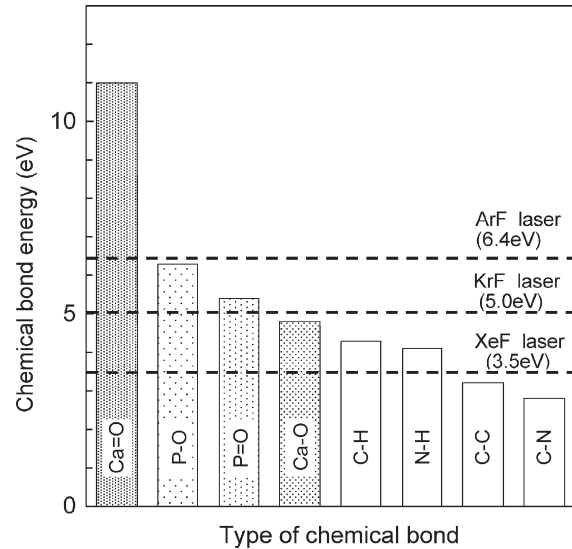


Fig. 7. Single photon energy levels of ArF, KrF and XeF excimer lasers and chemical bond energies of major components of hydroxyapatite and the bone.

(femurs) by KrF laser ablation. The result for sintered hydroxyapatite obtained in this study is higher than their result. According to their suggestion the organic component of the bone is ablated at the first stage and then this accelerates the ablation of the inorganic component (namely, hydroxyapatite) with lower laser fluence than the sintered hydroxyapatite, because most of the organic component of the bone showed lower chemical bond energy than the KrF as shown in Fig. 7.

XeF laser has the lowest photon energy in these excimer lasers and it is lower than the bond energies of major composition of hydroxyapatite. In this condition, photochemical ablation is difficult, and instead thermal ablation by melting and evaporating the surface layer occurred dominantly. This required higher threshold fluence, but resulted in much higher ablation rate than those of other 2 lasers. Thermal shock effect caused cracking at the edge of the hole as observed in Fig. 3(c) and their parts were scattered around the hole as in Fig. 3(a). Therefore, fine micro machining with XeF laser is difficult.

Debris around the hole are also affected by these different ablation phenomena; ArF laser showed very fine debris layer with amorphous hydroxyapatite. KrF laser showed the similar morphology, but including the coarse particles in the debris near the hole as apparently observed in Fig. 2 (b), and XeF showed large particles scattered as mentioned above.

#### 4. Summary

The effect of the photon energy of the excimer laser on the ablation rate and the surface morphology of the ablated area of a sintered hydroxyapatite sample has been examined by irradiating with three excimer lasers of ArF, KrF and XeF in air under normal atmospheric pressure. The results obtained are summarized as follows:

- (1) Photochemical ablation of a sintered hydroxyapatite is possible by using ArF and KrF excimer lasers due to

relatively higher photon energies than chemical bond energies of calcium or phosphorus with oxygen, and the flat bottom shape of an ablated hole with sharp edge can be obtained. On the contrary, thermal ablation occurred dominantly in the case of XeF laser due to low photon energy, and the ablated surface was rough and not flat with cracking at the edge of the hole.

- (2) The ablation rate of sintered hydroxyapatite for laser fluence was approximately 0.1, 0.2 and 28  $\mu\text{m}/\text{J}/\text{cm}^2$  for ArF, KrF and XeF lasers, respectively.
- (3) Threshold energy for the ablation of sintered hydroxyapatite was approximately 0.8, 1.5 and 6  $\text{J}/\text{cm}^2$  for ArF, KrF and XeF lasers, respectively.

### Acknowledgment

This work was supported by the Grant-in-Aid for Cooperative Research Project of Nationwide Joint-Use Research Institutes on Development Base of Joining Technology for New Metallic

Glasses and Inorganic Materials from The Ministry of Education, Science, Sports and Culture, Japan.

### References

- [1] P. Serra, L. Cleries, J.L. Morenza, *Appl. Surf. Sci.* 96–98 (1996) 216.
- [2] P. Serra, J.M. Fernandez-Pradas, G. Sardin, J.L. Morenza, *Appl. Surf. Sci.* 109–110 (1997) 384.
- [3] J.M. Fernandez-Pradas, G. Sardin, L. Cleries, P. Serra, C. Ferrater, J.L. Morenza, *Thin Solid Films* 317 (1998) 393.
- [4] P. Serra, J.L. Morenza, *Appl. Surf. Sci.* 127–129 (1998) 662.
- [5] V. Craciun, D. Craciun, P. Andreazza, J. Perriere, I.W. Boyd, *Appl. Surf. Sci.* 138–139 (1999) 587.
- [6] J.M. Fernandez-Pradas, L. Cleries, E. Martinez, G. Sardin, J. Esteve, J.L. Morenza, *Biomaterials* 22 (2001) 2171.
- [7] J.M. Fernandez-Pradas, M.V. Garcia-Cuenca, L. Cleries, G. Sardin, J.L. Morenza, *Appl. Surf. Sci.* 195 (2002) 31.
- [8] Y. Haraguchi, S. Hori, T. Nakayama, U. Kubo, *J. Fac. Sci. Technol., Kinki Univ.* 30 (1994) 149.
- [9] S. Fujisaka, T. Ito, K. Sato, *Rev. Laser. Eng.* 22 (1994) 402.